Direct Observations of the Cleavage Reaction of an L-DPPC Monolayer Catalyzed by Phospholipase A_2 and Inhibited by an Indole Inhibitor at the Air/Water Interface**

Xiuhong Zhai,[a, b] Junbai Li,*[a] Gerald Brezesinski,[b] Qiang He,[a] Helmuth Möhwald,*[b] Luhua Lai,[c] Ying Liu,[c] Liang Liu,[c] and Ying Gao[c]

The enzymatic hydrolysis of an L-dipalmitoylphosphatidylcholine (L-DPPC) monolayer at the air/water interface, catalyzed by phospholipase A_2 (PLA_2), serves as a model for biospecific interfacial reactions. The cleavage of L-DPPC was investigated by Brewster angle microscopy. Different types of domain defects were observed to form in the coexisting liquid expanded and liquid condensed phases during the hydrolysis reaction. The adsorption of the enzyme was quantitatively recorded as the increase of the surface pressure over a fixed molecular area with time. In the case of L-DPPC, the surface pressure first increases and then starts to decrease, which indicates that a soluble product (lysolipid) is produced during the catalytic cleavage reaction. The increase and decrease of the surface pressure, which corresponds to the change of shape and number density of domains, indicated the occurrence of the following processes: adsorption of PLA_2, cleavage reaction, and rearrangement of substrate and product molecules at the interface. Addition of a PLA_2 inhibitor to the lipid monolayer leads to a fast surface pressure increase after enzyme injection. The surface pressure reaches a maximum value and then does not change for a long time. During this period, no change in the domain shape and number density was observed, which indicates that the enzyme is inhibited for a certain period of time. The experimental results provide the possibility of a direct way to prove inhibitor activity.

KEYWORDS:

Brewster angle microscopy · enzymes · hydrolysis · inhibitors · phospholipids

Introduction

Phospholipase A_2 (PLA_2) is a calcium-dependent enzyme that exists in an extensive number of organisms. The enzymatic reaction of PLA_2 with the interface of a membrane consists of a molecular recognition process and a cleavage reaction.[1] PLA_2 stereoselectively hydrolyzes the sn-2 ester linkage of enantiomeric L-phospholipids to release fatty acids and lysophospholipids (Figure 1a). The activity of PLA_2 is 10000-fold greater at the interface of aggregated substrates, such as phospholipid monolayers at the air/water interface, compared to the reaction with the same substrate in its monomeric form.[2] In aqueous solution, PLA_2 has an α-helix-rich conformation (Figure 1b). A conformation change may occur during the enzymatic reaction as the enzyme reaches the interface.

Brewster angle microscopy offers a new prospect for direct visualization of the texture of Langmuir monolayers.[3] This technique allows characterization of the long-range orientational order of the assembly of a phospholipid monolayer that arises from the optical anisotropy induced by tilted aliphatic chains.[4] In the present work, this method is used to visualize the enzymatic cleavage reaction of L-DPPC monolayers and to verify the capacity of a selected inhibitor to inhibit the enzyme activity.

Results and Discussion

Adsorption and penetration of PLA_2

The enzyme-catalyzed hydrolysis of phospholipid monolayers consists of three main steps: enzyme adsorption and penetration, hydrolysis, and dissolution of the reaction products into the bulk phase. These three processes can be separated by studying

[a] *Prof. Dr. J. Li, X. Zhai, Q. He*
International Joint Lab
The Center for Molecular Science
Institute of Chemistry, Chinese Academy of Sciences
Zhong Guan Cun, Beijing 100080 (P.R. China)
Fax: (+86) 10-8261-2484
E-mail: jbli@infoc3.icas.ac.cn

[b] *Prof. Dr. H. Möhwald, X. Zhai, Dr. G. Brezesinski*
Max Planck Institute of Colloids and Interfaces
14476 Golm/Potsdam (Germany)
Fax: (+49) 331-5679-202
E-mail: moehwald@mpikg-golm.mpg.de

[c] *Prof. Dr. L. Lai, Dr. Y. Liu, Dr. L. Liu, Y. Gao*
Institute of Physical Chemistry
College of Chemistry and Molecular Engineering
Peking University, Beijing 100871 (P.R. China)

[**] *L-DPPC = L-dipalmitoylphosphatidylcholine.*

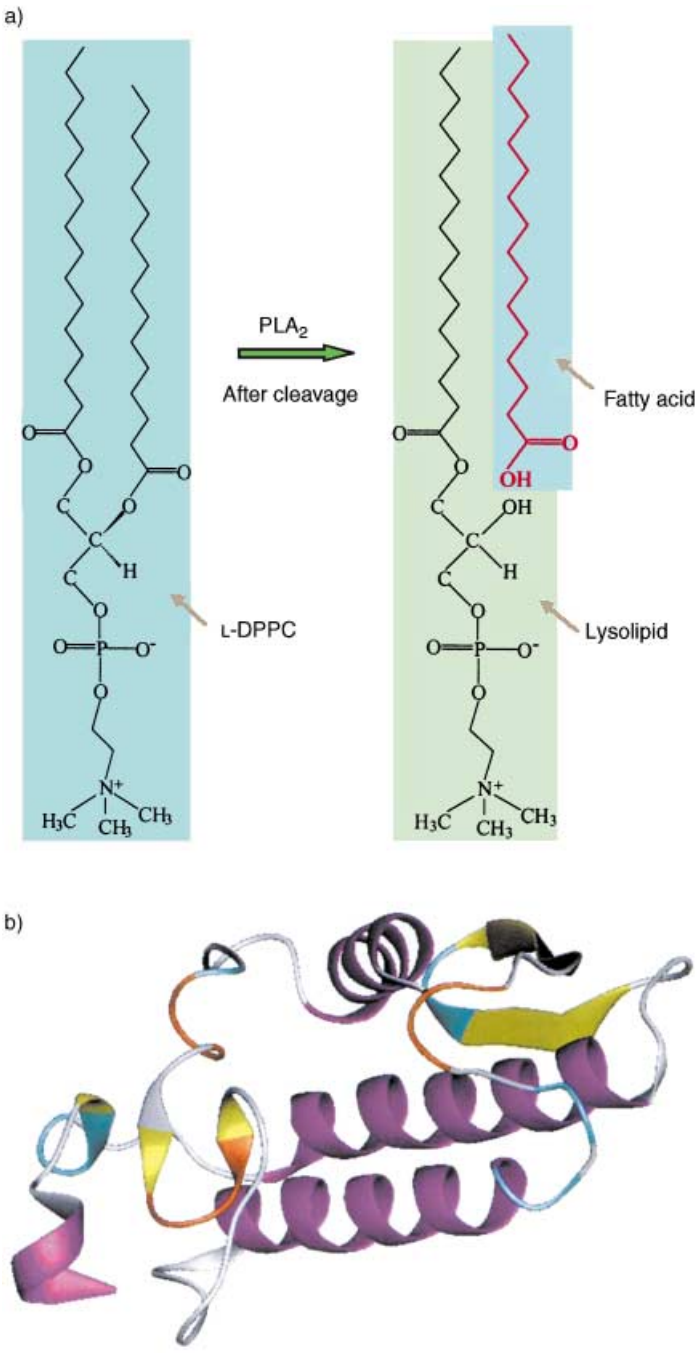

Figure 1. *a) Chemical structures of L-DPPC and the products of the PLA_2-catalyzed hydrolysis reaction. b) Ribbon representation of PLA_2.*

well-defined monolayers of enantiomeric phospholipids. PLA_2 is stereoselective and cannot hydrolyze D-dipalmitoyl-phosphatidylcholine (D-DPPC). The D-enantiomer can therefore be used to study the adsorption and penetration processes. Different methods were used to add PLA_2 to the D-DPPC system. One method used was injection of PLA_2 into the subphase at different initial monolayer pressures. If the phospholipid area is kept fixed, the surface pressure increases after PLA_2 injection as long as the initial surface pressure is not too high (8 mN m^{-1}, see Figure 2a). The maximum pressure is similar to that observed for a D-DPPC

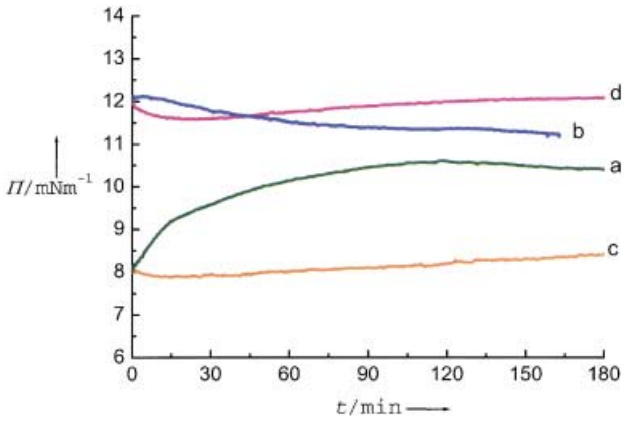

Figure 2. *Surface pressure of a D-DPPC monolayer as a function of time after injection of PLA_2 at initial surface pressures of (a) $\Pi_0 = 8$ mN m^{-1} and (b) $\Pi_0 = 12$ mN m^{-1}, and after spreading a D-DPPC monolayer onto the surface of a PLA_2 solution subphase and fast compression to (c) $\Pi_0 = 8$ mN m^{-1} and (d) $\Pi_0 = 12$ mN m^{-1}.*

monolayer after full expansion and recompression.[5] The enzyme starts to be squeezed out above 10 mN m^{-1}. Almost no change in surface pressure can be observed if the experiment starts at a higher initial surface pressure (12 mN m^{-1}). The reason for such behavior is the different penetration ability of PLA_2 at the higher pressure. If the monolayer is in a highly packed condensed state, PLA_2 is not able to penetrate into the monolayer phase.

The second method used for the additon of PLA_2 was to spread D-DPPC onto a PLA_2 solution. Immediately after spreading, the phospholipid monolayer was compressed to the initial surface pressure and the surface pressure was again measured as a function of time over a fixed molecular area. The $\Pi - t$ curves (Figure 2c) do not show any remarkable increase in pressure even if the initial surface pressure is 8 mN m^{-1}. However, the $\Pi - t$ curves observed on PLA_2 solution and those observed on the pure buffer solution at $\Pi_0 = 8$ and 12 mN m^{-1}, respectively (Figure 3), indicate a very weak PLA_2 adsorption and penetration

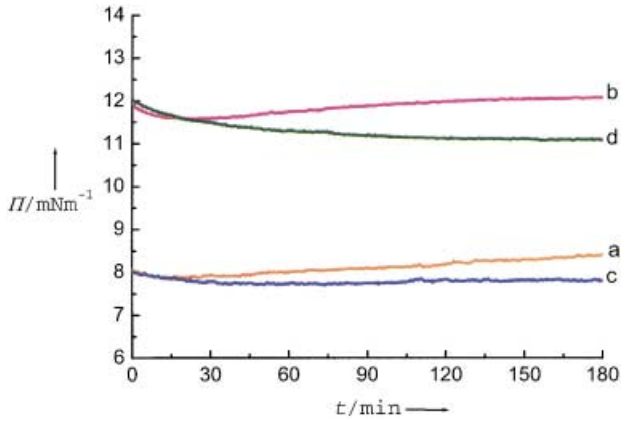

Figure 3. *Surface pressure as a function of time after spreading a D-DPPC monolayer onto the surface of a PLA_2 solution subphase and fast compression to (a) $\Pi_0 = 8$ mN m^{-1} and (b) $\Pi_0 = 12$ mN m^{-1}, and after spreading onto a buffer solution subphase and fast compression to (c) $\Pi_0 = 8$ mN m^{-1} and (d) $\Pi_0 = 12$ mN m^{-1}.*

after one hour. At lower surface pressure, close to the phase transition pressure, the different methods (injection or spreading) lead to different increases in the surface pressure. A possible explanation for such a phenomenon is that PLA_2 adsorption depends on local concentrations in the subphase. Injection of PLA_2 leads to initially inhomogeneous concentration profiles, and a locally high concentration of PLA_2 could accelerate the adsorption and penetration process.

In the case of L-DPPC, our measurements show that PLA_2 injection first causes an increase of surface pressure (Figure 4). The surface pressure increase directly after enzyme injection corresponds to adsorption and penetration of PLA_2 into the phospholipid monolayer. The adsorption rate depends on the initial pressure of the monolayer, we deduce that the process is faster at higher surface pressure. Brewster angle microscopy (BAM) experiments (Figure 5) show that a detectable cleavage reaction[6] starts after a few minutes (lag period). A comparison of Figure 4 and 5 indicates that the surface pressure increase takes at least 30 minutes, and after 30 minutes most of the domains are already cleaved and new domains with a different contrast effect are formed (Figure 5e). The lysophospholipid reaction product is at least partially soluble in the subphase. Therefore, the surface pressure increase as a result of enzyme penetration is limited because of dissolution of the lysophospholipid. However, the maximum pressure value is similar to or even higher than that in the D-DPPC system. This result indicates that the enzyme penetration is much faster and more pronounced than the dissolution of the reaction product. When the phospholipid solution is spread onto the PLA_2 subphase, there is again no enzyme penetration into the monolayer and the reaction leads immediately to the expected pressure decrease.

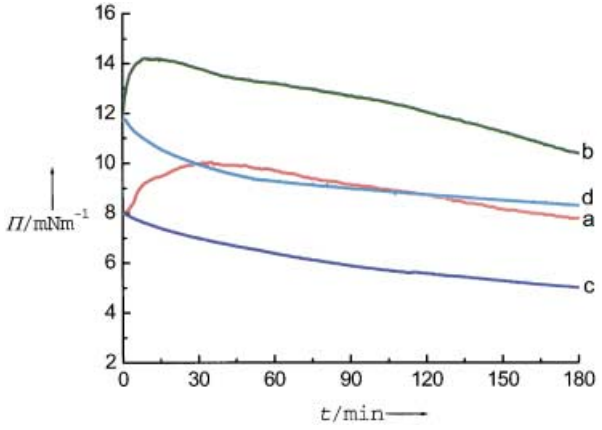

Figure 4. *Surface pressure of an L-DPPC monolayer as a function of time after injection of PLA_2 at initial surface pressures of (a) $\Pi_0 = 8\ mN\,m^{-1}$ and (b) $\Pi_0 = 12\ mN\,m^{-1}$, and after spreading of L-DPPC onto the surface of a PLA_2 solution subphase and fast compression to (c) $\Pi_0 = 8\ mN\,m^{-1}$ and (d) $\Pi_0 = 12\ mN\,m^{-1}$.*

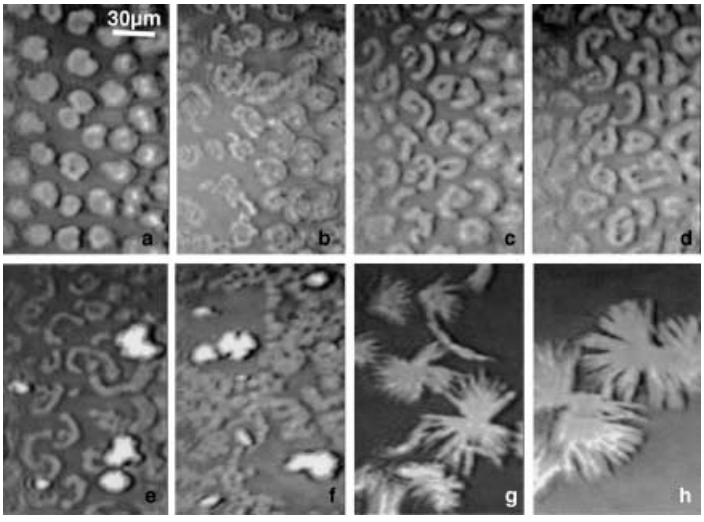

Figure 5. *BAM images of an L-DPPC monolayer cleaved by PLA_2. The images were taken 0 (a), 3 (b), 10 (c), 20 (d), 30 (e), 60 (f), 120 (g), and 180 (h) minutes after the hydrolysis reaction was started at $\Pi_0 = 7.5\ mN\,m^{-1}$.*

Direct observation of the cleavage reaction

Polarization-modulated infrared reflection absorption spectroscopy (PM-IRRAS) measurements of an L-DPPC monolayer revealed that PLA_2 has maximum activity in the presence of both the liquid expanded and liquid condensed (LE and LC) coexisting phases.[7] BAM experiments in this phase-transition region show that the cleavage reaction starts at the interface between the liquid-expanded phase and a condensed phase and proceeds into the condensed phase.[8] Packing defects are preferred places for the reaction. Depending on the sample history, the reaction starts either inside the domain or at the edge. Domains with inner damage, such as the "pizza" type domains, were observed 2 – 3 minutes after PLA_2 injection. This result demonstrated that in this case the reaction preferentially starts in the center of an LC domain.

Figure 5a – h shows the changes that occur in the L-DPPC domains after injection of the enzyme at an initial surface pressure of 7.5 $mN\,m^{-1}$. Three minutes after PLA_2 injection, two kinds of typical domain shapes were observed: C and O shapes (Figure 5b). The surface area of the domains decreases as a result of the cleavage reaction. The size of the C-shaped domains decreases drastically during the reaction but no change in shape occurs. The direction of hydrolysis in the C-shaped domains is assumed to be along the curvature of the domains. From this assumption, we deduce that the orientation of the molecules in the domain arms changes continuously and consequently follows the curvature of each arm.[9] The enzyme appears to preferentially catalyze hydrolysis in parts of condensed domains with the same molecular chain orientation. Figure 5d also shows O-shaped domains. This observation indicates that the enzyme has cleaved the central part of the domains, where the lipid molecules are less ordered because of the presence of defects. Finally, the domains can connect to each other and form a network structure.

A new kind of domain is observed about 30 minutes after enzyme injection (Figure 5e). The shapes of these domains are very different from those of L-DPPC domains. They have a relatively high reflectivity and are much brighter. The number of such domains increases with time. This process can be ascribed to the fact that either a product (fatty acid), the enzyme, or the

product–enzyme complex form their own domains. Such a phenomenon has also been observed in fluorescence microscopy investigations of the adsorption of a particular lung protein onto L-DPPC monolayers.[10] After 120 minutes, the new domains have aggregated and exhibit a star shape (Figure 5 g). The domains are surrounded by a fluid phase as a result of decreased surface pressure. To understand this transformation of the domains, we have to take into consideration the change of the line tension at the domain boundary caused by the presence of the enzyme,[11] and that the monolayer is now a mixture of substrate and reaction products. The monolayer structure was investigated by grazing incidence X-ray diffraction (GIXD) and is greatly affected by PLA_2 adsorption.[5] We used the D-enantiomer to show that the tilt angle of the aliphatic chains drastically decreases as a result of an enzyme-induced increase of the lipid packing density. This result indicates that the head-group structure (orientation and hydration), which determines the molecular area in condensed DPPC monolayers, changes because of interactions with the enzyme. GIXD measurement of the L-enantiomer takes too long to allow observation of changes due to adsorption. As discussed above, the reaction is evident after a short lag phase and leads to changes in the composition and therefore changes in the structure of the monolayer. Figure 6 shows a contour plot of diffracted intensity as a function of the in-plane and out-of-plane components of the scattering vector (Q) taken 2 h after starting the hydrolysis reaction at 20 mN m^{-1}. The diffraction pattern is rather complex. The typical reflections of a DPPC lattice, which is close to orthorhombic, can be seen. The tilt angle, as calculated from the Q_{xy} and Q_z data, is 31°. A tilt angle of 32.5° was observed in pure DPPC monolayers on the same buffer at 20 mN m^{-1}.[5a] These results show that the remaining DPPC is only slightly influenced by the presence of PLA_2. Additionally, a reflection that can be attributed to the hexagonal structure (condensed phase) of a phase-separated fatty acid appears at 1.525 Å^{-1}, which corresponds to a cross-sectional area of 19.6 Å^2. At such temperatures and pressures, palmitic acid exhibits a phase with a next-nearest-neighbor (NNN) tilt and a cross-sectional area slightly above 20 Å^2.[12] Interaction with either Ca^{II} ions or PLA_2 leads to tighter packing and the disappearance of the chain tilt. An additional Bragg peak at 1.415 Å^{-1} ($d = 4.44$ Å) shows that a third phase structure is present in the monolayer after the hydrolysis reaction. This structure must arise from a mixture of educt and product (most probably the lysolipid because the fatty acid forms its own phase-separated structure) under the influence of PLA_2. However, a single Bragg peak at nonzero Q_z values (Q_z = 0.25 Å^{-1}) cannot describe a monolayer structure. Therefore, either the second peak of an orthorhombic lattice is hidden by other peaks at zero Q_z (nearest neighbor tilted phase) or we expect to find another peak at $Q_z = 0.5$ Å^{-1} (NNN tilted phase), which did not appear in our measurements. When the first possibility is assumed to be the case, we find cross-sectional areas between 21.2 and 21.8 Å^2, which seem to be too large. Further experiments are needed to clarify this point.

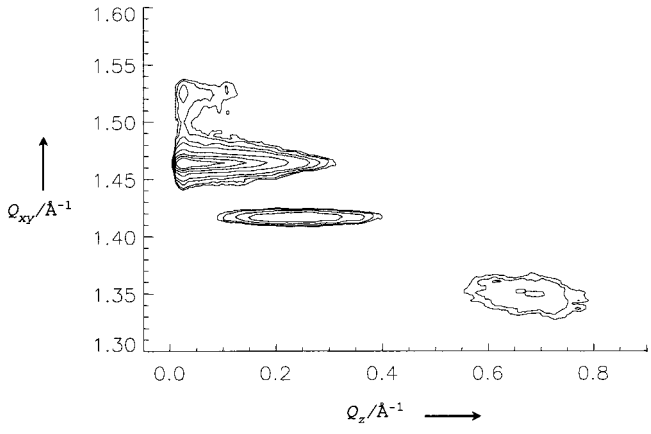

Figure 6. *Contour plot of the corrected X-ray intensity versus in-plane and out-of-plane scattering vector components Q_{xy} and Q_z of an L-DPPC monolayer after the hydrolysis reaction. The GIXD measurement was performed at 20 mNm^{-1}.*

To prove that the cleavage reaction mainly occurred in the LC phase, the monolayer was compressed to a higher surface pressure. Figure 7 shows the BAM images taken during the reaction with an initial surface pressure of 14 mN m^{-1}. At this pressure, the monolayer forms a homogeneous LC phase (Figure 7 a). After enzyme injection, morphology changes caused by the cleavage reaction were observed (Figure 7 b). Unlike the reaction in the two coexisting LC and LE phases, the cleavage reaction at this higher pressure took place at random positions in the monolayer. A homogeneous film was converted into a network film. The holes in the monolayer enlarge gradually and have irregular edges (Figure 7 c). At this higher pressure, enzyme and products began to form their own domains 80 minutes after injection (Figure 7 c–f).

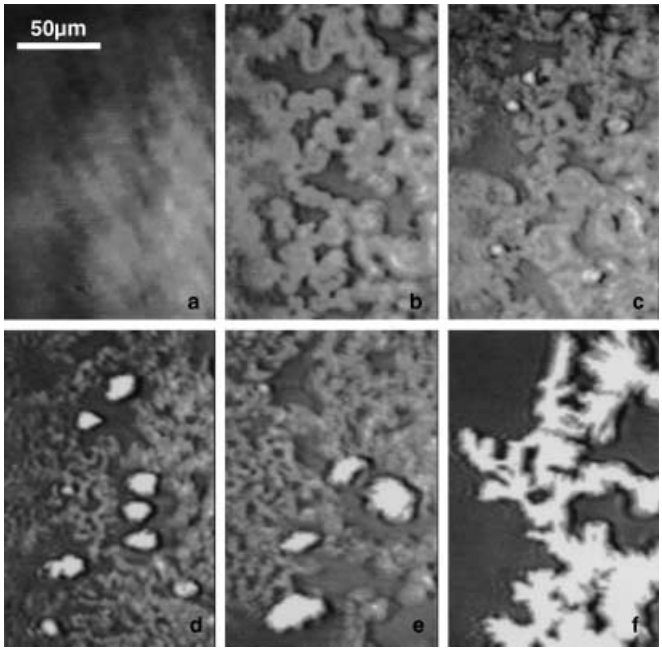

Figure 7. *BAM images of an L-DPPC monolayer cleaved by PLA_2. The images were taken 0 (a), 40 (b), 80 (c), 100 (d), 120 (e), and 200 (f) minutes after the hydrolysis reaction was started at $\Pi_0 = 14$ mN m^{-1}.*

Effect of a PLA_2 inhibitor on the cleavage reaction

The indole inhibitor 5-methoxy-2-methyl-1-(phenylmethyl)-1*H*-indole-3-acetamide is a typical inhibitor synthesized for human nonpancreatic secretory phospholipase A_2 and has an IC_{50} value (concentration required for 50% inhibition) of 0.84 ± 0.17 μM.[13] The inhibitor and L-DPPC were dissolved in chloroform in molar ratios of 5:1, 15:1, and 30:1, respectively, and then spread onto the air/subphase interface. The reason for such a procedure is the very low solubility of the inhibitor in the buffer used. Pure L-DPPC exhibits typical condensed-phase domains in the two-phase coexistence region at surface pressures between 6 and 8 mN m^{-1}. The addition of inhibitor spreads the pressure over larger molecular areas and leads to an increase of the phase transition pressure (Figure 8). The pure inhibitor does not form a

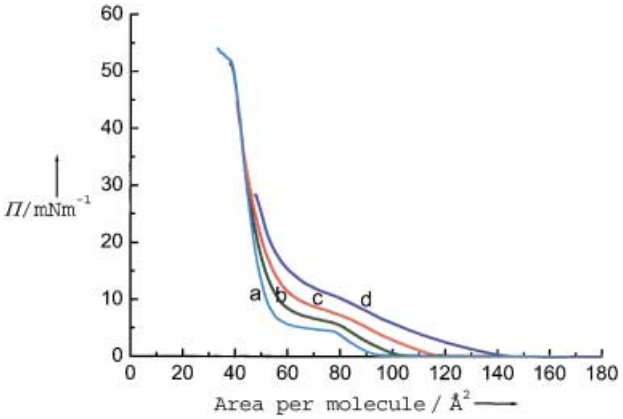

Figure 8. *Surface-pressure – area isotherms of pure L-DPPC (a) and of mixtures of inhibitor and L-DPPC at molar ratios of 5:1 (b), 15:1 (c), and 30:1 (d), respectively.*

stable monolayer on the buffer used in our PLA_2 experiments. In the isotherms presented in Figure 8, only the number of DPPC molecules has been taken into consideration for the calculation of the molecular area. The molecular area in the mixtures is shifted to larger values. Clearly, the surface area of the trough is partly occupied by the inhibitor. However, this area increase is much smaller than expected, which indicates that only a certain amount of the inhibitor remains on the surface as a result of interaction with DPPC molecules. Some inhibitor molecules must be dissolved or squeezed into the subphase. The remaining amount is clearly miscible with DPPC in the liquid-expanded phase and shifts the transition pressure to higher values. On compression, the inhibitor is completely squeezed out from the DPPC monolayer and at higher lateral pressures one observes the same molecular area as for pure DPPC. Circular domains similar to those of pure L-DPPC appear in the plateau region, which corresponds to the first-order phase transition of DPPC. However, the size of these domains (see below) is smaller than those of pure L-DPPC (Figure 5a). This observation supports our assumption that the inhibitor is miscible with fluid-like DPPC but not with DPPC in a condensed state.

Figure 9 shows the surface pressure as a function of time at a 30:1 molar ratio of inhibitor:L-DPPC. After PLA_2 injection into the subphase, the surface pressure increased very quickly in the first

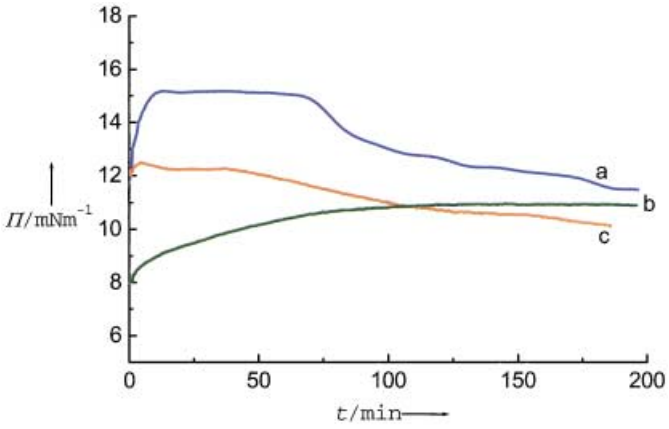

Figure 9. *Surface pressure as a function of time after injection of PLA_2. a) Mixture of inhibitor and L-DPPC at a molar ratio of 30:1, $\Pi_0 = 12$ mN m^{-1}; b) mixture of D-DPPC and L-DPPC at a molar ratio of 30:1, $\Pi_0 = 8$ mN m^{-1}; c) mixture of D-DPPC and L-DPPC at a molar ratio of 30:1, $\Pi_0 = 12$ mN m^{-1}.*

12 minutes. The domain shape remains unchanged for a long time after the injection of PLA_2 (Figure 10b – c). The surface pressure increase is slightly larger than that observed with pure L-DPPC (15 mN m^{-1} instead of 14 mN m^{-1}) and indicates that PLA_2 can penetrate into the mixed monolayer. In the case of the mixed monolayer, the surface pressure remains constant for more than one hour after reaching this maximum value. At the end of this plateau region in the $\Pi - t$ curve, the domains change shape, which indicates the start of the cleavage reaction. In contrast, the hydrolysis reaction was observed to start after a few

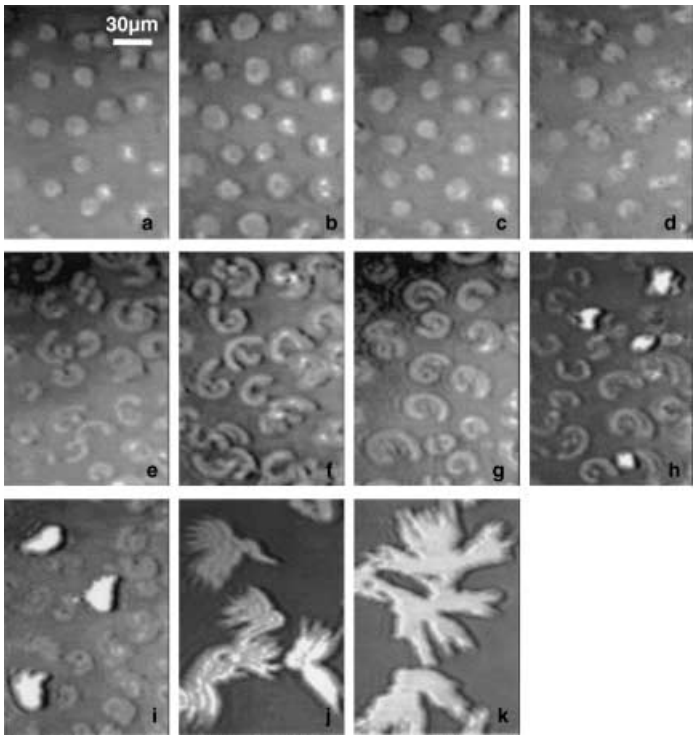

Figure 10. *BAM images of a mixed monolayer of inhibitor/L-DPPC (30:1) after injection of PLA_2. The images were taken 0 (a), 6 (b), 55 (c), 60 (d), 67 (e), 74 (f), 77 (g), 78 (h), 90 (i), 150 (j), and 180 (k) minutes after the hydrolysis reaction was started at $\Pi_0 = 12$ mN m^{-1}.*

minutes in pure L-DPPC monolayers (Figure 5b). This difference in time could be an indication of a certain degree of inhibition or simply connected with the drastically decreased amount of accessible L-DPPC molecules in the mixture. In order to distinguish these two possibilities, D-DPPC and L-DPPC were mixed in the same molar ratio of 30:1 and spread on the surface. The enzyme was injected in exactly the same way. The pressure–time curve produced is clearly different (Figure 9) from that of the L-DPPC/inhibitor mixture. There is only a little increase of the surface pressure after injection of PLA_2. D-DPPC is completely miscible with L-DPPC and cannot be cleaved. Therefore, the addition of D-DPPC leads only to a dilution of L-DPPC and reduces the reaction speed. The small concentration of L-DPPC in these mixtures means that the pressure decrease with time is mainly caused by relaxation of monolayer defects and only partly by the hydrolysis reaction, as can be seen by BAM. In contrast, the inhibitor can interact with PLA_2 in such a way as to cause the reaction to start much later. After 100 minutes, the two $\Pi - t$ curves have the same slope. How can one explain these findings? PLA_2 interacts preferentially with the inhibitor both at the surface and in the bulk solution. Figure 11 shows how the inhibitor can interact with the enzyme. A molecular design based on the combination of hydrogen bonds between inhibitor and enzyme shows possible connection modes (Figure 11a). Such an interaction may restrict the configuration variations of PLA_2 (Figure 11b) and result in a reduction of its activity.

Interactions between the inhibitor and PLA_2 could accelerate PLA_2 adsorption onto the surface and lead to the fast pressure increase observed. The plateau in the $\Pi - t$ curve (Figure 9) could then indicate a dynamic equilibrium between PLA_2 adsorption and desorption of the PLA_2/inhibitor complex. During this time, all the enzyme molecules reaching the surface are deactivated by the inhibitor and are therefore unable to catalyze the hydrolysis reaction. After 60 minutes, the first defective domains appeared (Figure 10d), which indicates the start of the hydrolysis reaction. During the next 30 minutes, all domains were partially cleaved. Mainly C-type domains (Figure 10e–g) appear during the hydrolysis. The surface pressure decrease reveals that a reaction product is soluble. The appearance of new domains with a much higher reflectivity could indicate that aggregates of PLA_2 and the fatty acid reaction product or aggregates of PLA_2 and the inhibitor are formed in the monolayer (Figure 10j–k). Since these domains appear at the end of the reaction and are very similar to those in Figure 5g–h, it seems more probable that the phase-separated fatty acid interacts with PLA_2 or Ca^{II} ions and forms these domains. Finally, the domains fuse to form larger domains surrounded by a fluid monolayer consisting of DPPC, lysolipid, and possibly remaining unreacted inhibitor.

Conclusions

The experiments reported herein use BAM to provide a visualization of the dynamic reactions that occur between PLA_2 and the different enantiomers of DPPC, as well as between PLA_2 and a mixture of L-DPPC with an inhibitor. Plots of pressure as a function of time show that the enzyme PLA_2 interacts much

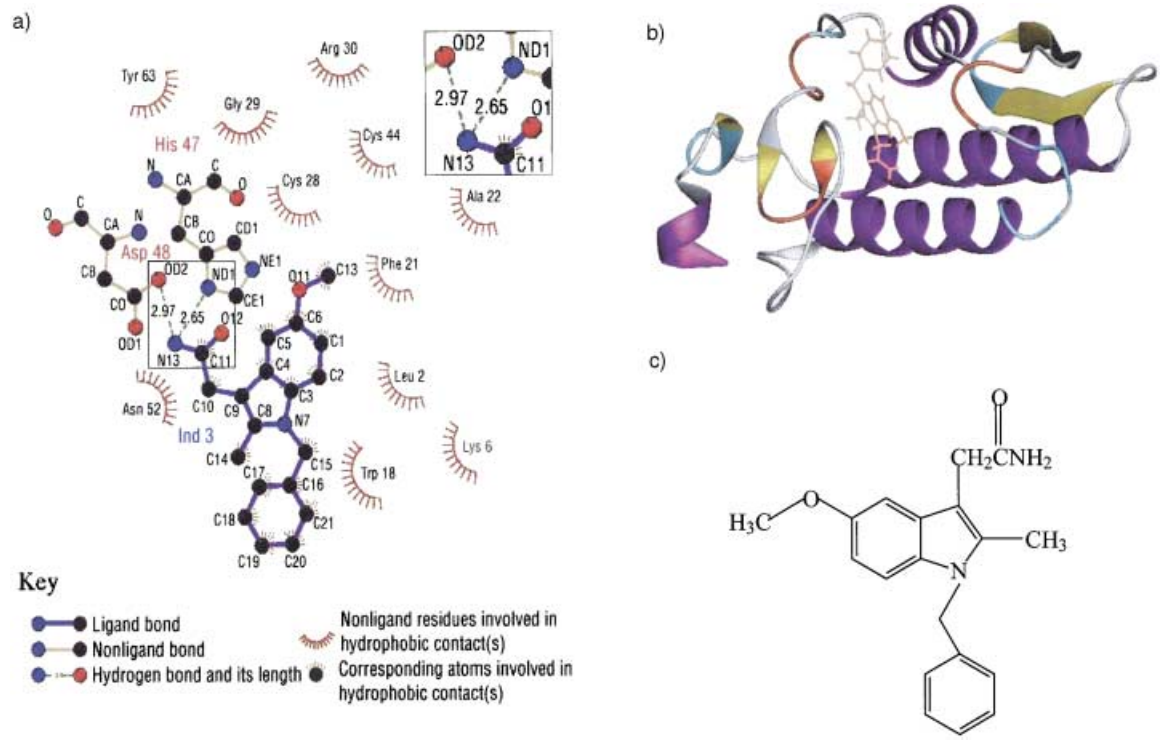

Figure 11. *a) Molecular design of a possible inhibitor binding pattern with PLA_2. The hydrogen bonds between the indole inhibitor and* Naja naja *PLA_2 are shown (finished with the Rasmol program; red balls represent oxygen atoms and blue balls represent nitrogen atoms). b) The position of the indole inhibitor in the active site of PLA_2 (modeled with the QUANTA program). The enzyme structure used in (a) and (b) has the Protein Data Bank (PDB) code 1POB and is the structure of PLA_2 of the Taiwan Cobra (*Naja naja atra*). c) Chemical structure of the indole inhibitor 5-methoxy-2-methyl-1-(phenylmethyl)-1*H*-indole-3-acetamide.*

more strongly with L-DPPC than with D-DPPC monolayers. The reactions with the two enantiomers are clearly different. The processes studied also depend on how the enzyme is introduced into the system (injection or spreading). This observation indicates that local concentration gradients play an important role.

The indole inhibitor used is to a certain extent miscible with liquid-like L-DPPC, but not with condensed DPPC. The transition pressure of DPPC is shifted to higher values in the mixtures, depending on the mixing ratio. The domains appearing in the transition range are smaller compared to those in the pure system but have the same shape. At high pressure, the inhibitor is squeezed-out from the DPPC monolayer. The inhibitor accelerates PLA_2 adsorption onto and penetration into the monolayer as a result of specific interactions and this process leads to a fast surface pressure increase. The indole inhibitor has a limited ability to inhibit the activity of PLA_2. The reaction starts much later than in pure L-DPPC or in L-DPPC/D-DPPC mixtures with the same molar fraction of L-DPPC as in experiments with the inhibitor.

Experimental Section

Materials: L-DPPC, D-DPPC, and phospholipase A_2 (from *Crotalus atrox* venom) were purchased from Sigma and used without further purification. The inhibitor, 5-methoxy-2-methyl-1-(phenylmethyl)-1*H*-indole-3-acetamide (see Figure 11 c) was synthesized based on a procedure described in ref. [12] and has been characterized by NMR and IR. The inhibitor is soluble in chloroform and has a very low solubility in water. Chloroform of at least 99% purity was purchased from ACROS. The water in all experiments was purified by use of a Milli-Q system.

Methods:

Langmuir monolayers: Monolayers of the pure enantiomers or of lipid mixtures were prepared from phospholipid/chloroform solutions (1 mM) on a buffer subphase (pH 8.9) containing NaCl (150 mM), $CaCl_2$ (5 mM), and tris(hydroxymethyl)aminomethane (10 mM). After evaporation of the solvent, pressure – area isotherms were measured on a Langmuir trough (R&K, Wiesbaden, Germany) equipped with a Wilhelmy-type pressure measuring system. In all experiments, the compression rate was 2.5 $Å^2$ molecule^{-1} min^{-1}. To follow the cleavage reaction, the monolayer was compressed to a suitable initial pressure and the enzyme was injected into the subphase with a tiny syringe, or a monolayer was spread onto the PLA_2 subphase and quickly compressed to the initial pressure. The final PLA_2 concentration was 0.12 units mL^{-1}. The temperature was $20 \pm 0.1\,^{\circ}C$. Changes in area or pressure as well as of monolayer morphology were simultaneously recorded.

Brewster angle microscopy: A commercial BAM instrument (Optrel, Germany) was mounted onto the computer-interfaced Langmuir trough. The reflected light was detected by an analyzer and a CCD camera. The output signal was recorded on a high-quality video recorder. The images were captured afterwards through a frame grabber and processed by using the software of COMPIC to adjust the contrast and to correct the image distortion that results from observation at the Brewster angle.

Synchrotron X-ray diffraction: GIXD experiments were performed by using the liquid-surface diffractometer on the undulator beamline BW1 at the Hamburger Synchrotronstrahlungslabor at the Deutsches Elektronen-Synchrotron (Hamburg, Germany). A monochromatic synchrotron beam strikes the air/water interface at grazing incidence angle $\alpha_i = 0.85\alpha_c$, where α_c is the critical angle for total external reflection. The diffracted intensity is detected by a linear position-sensitive detector (PSD; OED-100-M, Braun, Garching, Germany) as a function of the vertical scattering angle α_f. A Soller collimator is located in front of the PSD and provides the resolution for the horizontal scattering angle $2\theta_{xy}$. The horizontal (in-plane) component of the scattering vector Q is given by $Q_{xy} \approx (4\pi/\lambda)\sin(\theta_{xy})$ and the vertical (out-of-plane) component is given by $Q_z \approx (2\pi/\lambda)\sin(\alpha_f)$, where λ is the X-ray wavelength.[14] The diffracted intensities were corrected for polarization, effective area, and the Lorentz factor. Model peaks taken to be Lorentzian in the in-plane direction and Gaussian in the out-of-plane direction were fitted to the corrected intensities. From the peak positions we could obtain the lattice parameters and the tilt angle.

We acknowledge the financial support of the National Nature Science Foundation of China (Grant no. NNSFC29925307), the Major State Basic Research Development Program (973, Grant. no. G2000078103), and the Chinese Academy of Sciences, as well as the collaboration on the project of the German Max Planck Society.

[1] a) J. J. Janda, E. J. Bottone, *J. Clin. Microbiol.* **1981**, *14*, 55 – 60; b) M. H. Gelb, M. K. Jain, O. Berg, *Bioorg. Med. Chem. Lett.* **1992**, *2*, 1335 – 1342; c) R. Verger, G. H. de Haas, *Chem. Phys. Lipids* **1973**, *10*, 127 – 136.

[2] a) R. Verger, M. C. E. Mieras, G. H. de Haas. *J. Biol. Chem.* **1973**, *248*, 4023 – 4034; b) M. Menashe, D. Lichtenberg, C. Gutierrez-Merino, R. L. Biltonen, *J. Biol. Chem.* **1981**, *256*, 4541 – 4543; c) T. L. Hazlett, E. A. Dennis, *Biochemistry* **1985**, *24*, 6152 – 6158.

[3] a) S. Hénon, J. Meunier, *Rev. Sci. Instrum.* **1991**, *62*, 936 – 939; b) D. Hönig, D. Möbius, *J. Phys. Chem.* **1991**, *95*, 4590 – 4592; c) V. Melzer, D. Vollhardt, *Phys. Rev. Lett.* **1996**, *76*, 3770 – 3773.

[4] a) T. M. Fischer, R. F. Bruinsma, C. M. Knobler, *Phys. Rev.* **1994**, *50*, 413 – 428; b) G. Weidemann, G. Brezesinski, D. Vollhardt, D. DeWolf, H. Möhwald, *Langmuir* **1999**, *15*, 2901 – 2910; c) C. M. Knobler, D. K. Schwartz, *Curr. Opin. Colloid Interface Sci.* **1999**, *4*, 46 – 51.

[5] a) U. Dahmen-Levison, G. Brezesinski, H. Möhwald, *Thin Solid Films* **1998**, *327 – 329*, 616 – 620; b) D. W. Grainger, A. Reichert, H. Ringsdorf, C. Salesse, *FEBS Lett.* **1989**, *252*, 73 – 82.

[6] D. W. Grainger, A. Reichert, H. Ringsdorf, C. Salesse, *Biochim. Biophys. Acta.* **1990**, *1023*, 365 – 372.

[7] D. Blaudez, T. Buffeteau, J. C. Cornut, B. Desbat, N. Escafre, M. Pezolet, J. M. Turlet, *Appl. Spectrosc.* **1993**, *47*, 869 – 874.

[8] a) J. B. Li, Z. J. Chen, X. L. Wang, G. Brezesinski, H. Möhwald, *Angew. Chem.* **2000**, *112*, 3187 – 3191; *Angew. Chem. Int. Ed.* **2000**, *39*, 3059 – 3062; b) U. Dahmen-Levison, G. Brezesinski, H. Möhwald, *Prog. Colloid Polym. Sci.* **1998**, *110*, 269 – 274.

[9] a) R. M. Weis, H. M. McConnell, *Nature* **1984**, *310*, 47 – 49; b) G. Weidemann, D. Vollhardt, *Colloids Surf. A* **1995**, *100*, 187 – 202.

[10] M. M. Lipp, K. Y. C. Lee, J. A. Zasadzinski, A. J. Waring, *Science* **1996**, *273*, 1196 – 1199.

[11] a) M. Seul, D. Andelmann, *Science* **1995**, *267*, 476 – 483; b) H. M. McConnell, V. T. Moy, *J. Phys. Chem.* **1988**, *92*, 4520 – 4525; c) H. Haas, H. Möhwald, *Thin Solid Films* **1989**, *180*, 101 – 110.

[12] V. M. Kaganer, H. Möhwald, P. Dutta, *Rev. Mod. Phys.* **1999**, *71*, 779 – 819.

[13] R. D. Dillard, N. J. Bach, S. E. Draheim, D. R. Berry, D. G. Carlson, N. Y. Chirgadze, D. K. Clawson, L. W. Hartley, L. M. Johnson, N. D. Jones, E. R. McKinney, E. D. Mihelich, J. L. Olkowski, R. W. Schevitz, A. C. Smith, D. W. Snyder, C. D. Sommers, J. Wery, *J. Med. Chem.* **1996**, *39*, 5119 – 5136.

[14] a) K. Kjaer, *Phys. B* **1994**, 198, 100 – 109. b) J. Als-Nielsen, D. Jacquemain, K. Kjaer, M. Lahav, F. Leveiller, L. Leiserowitz, *Phys. Rep.* **1994**, *246*, 251 – 313; b) R. Rietz, W. Rettig, G. Brezesinski, W. G. Bouwman, K. Kjaer, H. Möhwald, *Thin Solid Films* **1996**, *284*, 211 – 215.

Received: November 8, 2002 [F 526]